IEEE Photonics Journal
An IEEE Photonics Society Publication

Open Access

Far-Infrared Circular Polarization and Polarization Filtering Based on Fermat's Spiral Chiral Metamaterial

Volume 7, Number 3, June 2015

Natesan Yogesh
Tao Fu
Feng Lan
Zhengbiao Ouyang

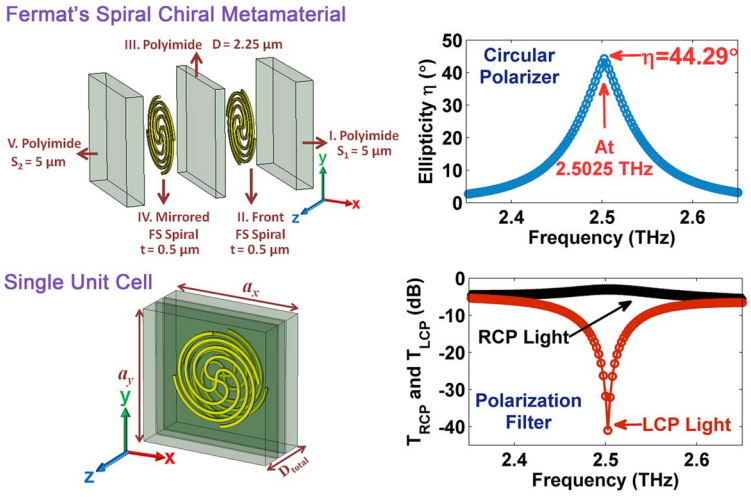

DOI: 10.1109/JPHOT.2015.2423291

IEEE photonics SOCIETY

IEEE

Far-Infrared Circular Polarization and Polarization Filtering Based on Fermat's Spiral Chiral Metamaterial

Natesan Yogesh,[1] Tao Fu,[1] Feng Lan,[2] and Zhengbiao Ouyang[1]

[1]Solid State Photonics Laboratory, THz Technical Research Center, Shenzhen Key Laboratory of Micro-Nano Photonic Information Technology, Key Laboratory of Optoelectronic Devices and Systems of the Ministry of Education and Guangdong Province, College of Electronic Science and Technology, Shenzhen University, Shenzhen 518060, China
[2]School of Physical Electronics, University of Electronic Science and Technology of China, Chengdu 610054, China

DOI: 10.1109/JPHOT.2015.2423291

Manuscript received February 28, 2015; revised April 3, 2015; accepted April 10, 2015. Date of publication April 30, 2015; date of current version May 6, 2015. This work was supported in part by the National Science Foundation of China under Grant 61275043 and Grant 60877034, by the Guangdong Province National Science Foundation under Key Project Grant 8251806001000004, and by the Shenzhen Science Bureau under Grant 200805 and Grant CXB201105050064A. Corresponding author: Z. Ouyang (e-mail: zbouyang@szu.edu.cn).

Abstract: A bilayered-twisted Fermat's spiral chiral metamaterial (FSCMM) is proposed for the realization of circular polarization of far-infrared waves and polarization filters. It is demonstrated through full-wave simulations that the proposed FSCMM can convert waves from linear to circular polarization (CP) around 2.5 THz. The reported FSCMM is sensitive to the handedness of circularly polarized light, where it can filter out either right-handed or left-handed CP light with an optical isolation of 35 dB around 2.5 THz. The proposed FSCMM is compact with a dimension of $\lambda/4 \times \lambda/4 \times \lambda/9$ at the far-infrared operating waveband. The CP conversion and filtering functionalities of the proposed FSCMM are ensured for oblique incidences up to 20° with an optical isolation of more than 25 dB for both *x*- and *y*-oriented linear polarized excitations. The operation bandwidth of the proposed system is enhanced in the level of 0.058 THz to 0.11 THz for two- and three-unit-cell composite systems, respectively. Due to the strong circular dichroism, compactness, wide-angle functionalities, and appreciable bandwidth, the proposed FSCMM is useful for the development of integrated far-infrared spectroscopic and imaging devices.

Index Terms: Metamaterials, terahertz, far infrared.

1. Introduction

Tailoring the polarization state of any electromagnetic radiation is fundamental in all branches as it is a phenomenal tool for probing the matter properties. In particular, the manipulation of terahertz (THz) waves in the form of linear and circular polarizations is important in modern day photonic devices in imaging, scanning, and communication sciences [1]–[3]. For example, THz radiation in the far-infrared spectrum (0.5 THz to 12 THz) is proven to be a powerful imaging tool [4] in chemistry, biology and astronomy, as many chemical species and biological samples are showing molecular resonance at these frequencies. Developing circular polarizers and dichroic filters at this regime further enables the probe of optical activity of chemical and biological

samples. Moreover, polarization filters are useful in eliminating background noise and promoting the sensitivity of biomedical signal detection as organic molecules are handed, and they interact strongly with light waves for a certain kind of polarization.

It is known that for circular polarization (CP) conversion and filtering functionalities of THz radiation, one can rely on several conventional optical components such as Fresnel rhomb [5], prisms [6], and wire-grid polarizers [7], [8]. It is noted that in these devices, the 90° phase difference between transverse electric (TE) and transverse magnetic (TM) polarization components is produced via total internal reflection (TIR) so that the output is a circularly polarized light. Even though the devices based on TIR are feasible for broadband operation with high transmission, the bulky nature precludes the design of compact circular polarizers at far-infrared frequencies. For example, the typical size of a Fresnel rhomb requires the dimension of 10 mm $\times$ 10 mm $\times$ 10 mm for the design wavelength of 587.6 nm (FRB-1010-4, Sigma-Koki™). On the other hand, the prism-based devices [6] require precise index contrast for CP conversion over the operation wavelength.

Apart from TIR-based devices, birefringent materials are optically active materials, which show different phase velocities and refractive indices along crystallographic axes. The quarter wave retarder (QWR) formed by birefringent material is a thickness-dependent device, where the CP conversion relies on the path difference of $\lambda/4$. However, absorption loss is one of the disadvantages of birefringent materials at THz bands. In earlier days, magneto-optical crystals like Indium antimonide (InSb) was also used for CP conversion at far-infrared frequencies, but it requires external applied magnetic field [9]. Meanderline structures [10], [11] are another important category of THz CP devices, in which the inductive and capacitive effects of the metal structures show necessary phase shift and amplitude requirement for CP conversion. In [11], CP conversion is achieved around 0.64 THz with an operating bandwidth of 0.128 THz.

Recently, the advent of chiral metamaterials (CMM) offers another avenue to realize functional THz polarization devices [12]. Chiral metamaterials are artificial electromagnetic structures that lack mirror symmetry along the direction of propagation and could entail huge optical activity and circular dichroism [13], [14]. Helices are the foremost artificial chiral structure, as Lindman demonstrated its optical activity at microwave frequencies [15], [16]. Until now, helices are the best candidates for the design of circular polarizers even at THz and visible frequencies owing to its larger circular dichroism, broadband operation and higher optical isolation [17]–[19]. However, fabrication complexity is the major drawback of helical structures at micro and nano length scales.

Apart from helices, other chiral structures are identified into two broad categories based on length scales. If the applied wavelength is comparable to the periodicity of the chiral constituents, the structures are defined as chiral photonic crystals (CPhCs). Circular polarizers and beam splitters could be realized using CPhCs in 3-D structures with chiral nets [20], rotational stacks [21], [22], and bi-chiral systems [23]. Other than CPhCs, metal-hole arrays [24] are non-chiral systems and rely on birefringence characteristics for CP conversion. Diffraction orders, efficiency, and fabrication difficulties are the challenges of periodic structures in CP device realization. The second category of chiral structures operating in the homogenization limit (i.e., the wavelength being much greater than the period in the structures) is also investigated extensively. Several bi-layered enantiomeric metallic patterns embedded in dielectric substrates have been reported for CP conversion at microwave frequencies in the form of U-shaped split-ring resonators (U-SRR) [25], [26], wheel pattern [27], twisted double SRR [28], meta surfaces [29], Hilbert tiles [30], bisected arc [31], connected squares [32] and so on. At microwave frequencies, these CMM structures are extremely thin and metal can behave as a perfect conductor. However at THz wavelength scales, thick metal is one of the major problems in reducing the device functionality. Hence for direct scaling to THz frequencies, the CMM must exhibit strong circular dichroism in the presence of thick metal. For example, a bi-layered U-SRR possesses strong circular dichroism due to its supramolecular chirality in which each layer of U-SRR itself is chiral in nature [25], [26] and hence it is suitable for direct scaling to far-infrared frequencies.

Kenanakis group implemented this structure in standard layer-by-layer method and demonstrated its CP conversion at 4.2 THz [33]. However, it is noticed that further down scaling the CP resonance below 4.2 THz requires larger lateral dimensions of a unit cell. This leaves further scope for achieving the compact design. At the same time, in microwave frequencies, the wheel pattern [27], twisted double SRR [28], Hilbert tiles [30] and connected square patterns [32] dealt the compactness problem extensively. However, circular dichroism of these structures is similar and even low with respect to U-SRR and its asymmetric form [25], [26], and they would result in low optical isolation upon THz scaling.

Other than compactness and strong chirality, the problem of incident angle compatibility is rarely investigated. For example, structures like bisected arc [31] and non-chiral MTM [34] possess extrinsic chirality and their optical activity exists only for certain polarization of incident field and non-normal incidences. Therefore, relying on anisotropy property due to off-normal incidences will reduce the wide angle functionality of circular polarizer designs.

Broadband operation is another important requirement for practical implementation of CP devices. However, whatever the designs may be (including the one reported in the present paper), planar structures with disconnected lattices are not appropriate for broadband operation. In 3-D counterpart, metafoils [35] are proposed for wideband operation but the fabrication of this structure requires more facilities than layer-by-layer method. However, within the scope of the planar structure, bandwidth can be enhanced through multiple stacking of unit cells by gradually varying the geometrical dimensions. For example, in [36], a cut-wire pair is gradually rotated along the direction of propagation of light, so that the composite structure will mimic a helix. In this method, broad bandwidth is achieved but the optical isolation is low. On the other hand, the unit cell parameter variation (such as gap width variation) would result in minute shift in resonance frequency and thus minimal bandwidth (e.g., 0.022 GHz in [27]). Since more cells would result in greater loss in this method, bandwidth increment is obtained at the cost of higher loss and larger thickness.

In this paper, we propose a bilayered-twisted Fermat's spiral chiral metamaterial (FSCMM) for the realization of far-infrared circular polarizer and polarization filter with the objectives of higher optical isolation, compactness, wide angle operation including the bandwidth requirements. The proposed single-unit-cell FSCMM exhibits strong circular dichroism with an optical isolation of 35 dB around 2.5 THz. The coupling mechanism consists of both anti-symmetric magnetic dipole and symmetric electric dipole interactions so that the FSCMM will convert the linearly polarized light into circularly polarized light through the induction of equal magnitude of cross- and co-polarized fields. The strong capacitive coupling between the adjacent rings enables the functionality for oblique incidences. Together with CP conversion, FSCMM also shows circular polarization filtering functionalities, where one can design right- (RCP) and left-handed circular polarization (LCP) filters based on the handedness of the FSCMM structure. The bandwidth of CP conversion and filtering functionalities is enhanced through the composite system by tailoring the functional dependence of FS patterns.

2. Design Principle and Optical Activity of Proposed FSCMM

Fig. 1 shows the design principle and unit cell construction of proposed FSCMM. Fermat's spiral (FS) shown in Fig. 1(a) has the functional dependence of $r = A\sqrt{\theta}$, where A is the spiral parameter representing the degree of spiraling for the given number of turns. FS spiral is chosen for the CMM design because it is more compact than the normal Archimedean spiral $(r = A\theta)$. For example, for a given value of spiral constant and a spiral turn of 2π, the average diameter of Fermat's spiral is two times less than the normal spiral. This aspect significantly reduces the transverse dimension of the unit cell required for far-infrared realization.

In Fig. 1(b), a quadfilar system is built by placing four FS arms with 90° rotational arrangement. Each spiral shown in Fig. 1(b) has a spiral turn of 2π and the spiraling constant of $A = 4.8\ \mu\text{m}/\sqrt{\text{rad}}$ is taken in the designs of CMMs. In general, the quadfilar system will be preferred for the design of CP converters because the eigenstates of C_4 symmetry systems are pure

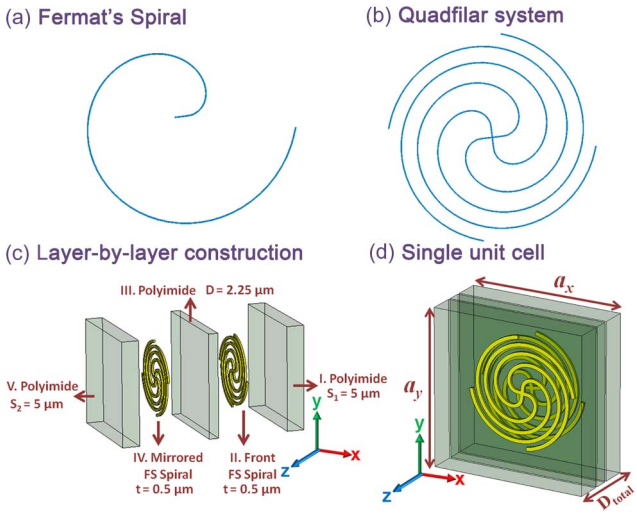

Fig. 1. Unit cell of a proposed THz Fermat's spiral chiral metamaterial. (a) Single strand of FS pattern. (b) Quadfilar arrangement of FS pattern. (c) Layer-by-layer construction of a unit cell. (d) Geometry of one unit cell. THz radiation is incident from S_1 side.

circular polarizations (RCP and LCP light), and mixed polarizations are forbidden due to the symmetry. The quadfilar system is traced out in metal with the thickness of $t = 0.5$ µm and width of $w = 0.7$ µm. The chiral pattern is formed by mutually conjugated quadfilar systems so that the combination breaks the mirror symmetry along the direction of propagation of light.

The CMM design is implemented in standard layer-by-layer method using polyimide spacers and substrates as shown in Fig. 1(c). Polyimide has a dielectric constant of 2.9 and the flexible thin sample has a high transmission of more than 95% in the frequency range of 0.2 THz to 2.5 THz [37]. As per the layer-by-layer method, the first layer is started with a polyimide spacer thickness of $S_1 = 5$ µm. This choice of supportive spacer thickness is feasible with the spin-coating of liquid polyimide such as Dupont Pyralin PI-2525 [33] and PI-5878G [37]. The second layer is the FS metal pattern, which has a thickness of $t = 0.5$ µm. The metal is modeled with lossy silver with the conductivity of $\sigma = 6.3012e7$ S/m. The third layer is the polyimide dielectric substrate of thickness $D = 2.25$ µm. The fourth layer is the backside FS spiral, which is a conjugated form of the second layer. The dielectric substrate thickness $D = 2.25$ µm mainly controls the electromagnetic interaction between the front and backside FS patterns. It is useful to mention that though the choice of this substrate thickness has high accuracy, the state of art spin coating method can go up to sub-micron thickness tolerance, and this choice can be considered for desirable target thickness in modeling and fabrication process. The fifth layer is the supportive polyimide spacer of thickness $S_2 = 5$ µm. The combined single unit cell shown in Fig. 1(d) has a total thickness $D_{\text{total}} = 13.25$ µm. Lattice constants of the unit cell are taken as $a_x = a_y = 30$ µm.

Optical activity of the proposed FSCMM is solved through full-wave electromagnetic simulations using CST Microwave Studio with frequency domain calculations. Unit cell boundary conditions are applied along x and y directions of FSCMM unit cell [see Fig. 1(d)], and perfectly matched boundary layers are set along the z direction. In Floquet port analysis, transmission coefficients are computed in the frequency range of 2 THz to 4.5 THz for both x- (TM) and y-polarized (TE) modes.

For the process of linear to circular polarization, the CMM structure should possess equal magnitude of cross- and co-polarized transmissions and the phase difference between these transmissions must be odd integer multiples of 90°. The cross- and co-polarization transmissions are defined as $T_{xy} = E_x^t/E_y^i$ and $T_{yy} = E_y^t/E_y^i$ accordingly, where E_y^i is the electric field of the y- polarized incident wave, and E_x^t and E_y^t are the x and y components of the transmitted

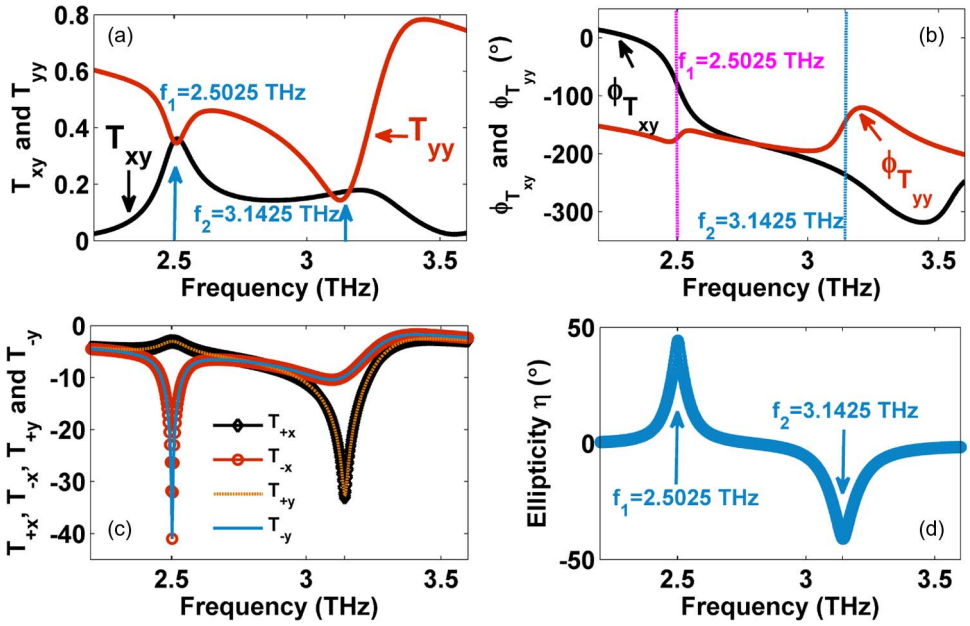

Fig. 2. (a) and (b) Corresponding to the amplitude and phase spectrum of cross- and co-polarized transmission levels of the FSCMM, respectively. (c) Circular polarization transmissions plot for *x*- and *y*-polarized normal incident light and (d) the corresponding ellipticity spectrum.

electric fields, respectively. It may be noticed that in the absence of chirality, there will be no cross-polarization transmission as $T_{xy} = 0$. To compute the CP transmission and ellipticity parameter, Jones matrix is constructed in the circular polarization basis [28] as follows:

$$\begin{pmatrix} E_+^t \\ E_-^t \end{pmatrix} = \frac{1}{\sqrt{2}} \begin{pmatrix} T_{+x} & T_{+y} \\ T_{-x} & T_{-y} \end{pmatrix} \begin{pmatrix} E_x^i \\ E_y^i \end{pmatrix} \tag{1}$$

$$\begin{pmatrix} T_{+x} & T_{+y} \\ T_{-x} & T_{-y} \end{pmatrix} = \begin{pmatrix} T_{xx} + iT_{yx} & T_{xy} + iT_{yy} \\ T_{xx} - iT_{yx} & T_{xy} - iT_{yy} \end{pmatrix} \tag{2}$$

$$\eta = \arctan \frac{|E_+| - |E_-|}{|E_+| + |E_-|} \tag{3}$$

where E_+^t and E_-^t are the transmission of right-handed (RCP) and left-handed (LCP) circular polarized waves, respectively, E_x^i and E_y^i are the *x*- and *y*-oriented linearly polarized incident waves, respectively, $T_{+x}(T_{-x})$ and $T_{+y}(T_{-y})$ are the RCP (LCP) waves corresponding to *x*- and *y*-oriented linearly polarized incident waves respectively, and η is the ellipticity of transmitted light. It is noted that $\eta = 45^\circ$ corresponds to pure circularly polarized light.

Fig. 2 shows the circular dichroism results of the proposed FSCMM. From Fig. 2(a), one can observe that there are two frequency points, which satisfy the condition of equal magnitude of T_{xy} and T_{yy}. At $f_1 = 2.5025$ THz, the magnitudes of T_{xy} and T_{yy} are of the order of 0.35. Similarly at $f_2 = 3.1425$ THz, the magnitudes of T_{xy} and T_{yy} are of the order of 0.16. From Fig. 2(b), it is observed that at f_1 and f_2, the phase difference between T_{xy} and T_{yy} is found to be 90.32° and -91.2°, respectively. Though both frequencies satisfy the CP conversion condition, the amplitude strength of the second frequency (f_2) is very low and hence this frequency is not suitable for device implementation. On the other hand, the first frequency $f_1 = 2.5025$ THz shows higher transmission even at the cost of impedance mismatch due to polyimide substrate and it is more suitable for CP converter implementation.

The circular transmission coefficients are plotted in Fig. 2(c) for *x*- and *y*-oriented normal incident linear polarized waves. It is observed that the RCP transmissions for both *x*- and

y-polarized incidences are found to be $T_{+x} = T_{+y} = -3.04$ dB at 2.5025 THz. The corresponding ellipticity is 44.29° at 2.5025 THz, which indicates that the output is a pure circularly polarized light. Suppose the dielectric constants of substrate and spacers are less than 2.9, impedance mismatch can be further reduced and hence the RCP transmission loss could be minimized to be less than 3 dB. However, it is noticed that the choice of the substrate not only depends on the dielectric constant but requires considerations on other experimental aspects as well, such as the planarization and conformal metal adhesion [38] so that the material is compatible under layer-by-layer construction. Under these aspects, polyimide is chosen as a suitable substrate than other low dielectric substrates such as PVDF and Teflon at far-infrared frequencies. This choice restricts the CP conversion transmission level at around 3 dB for the unit cell thickness of 13.25 μm including the spacers. On the other hand, if one removes the spacers, the standalone FSCMM structure shows an RCP insertion loss of 1.6 dB for the substrate dielectric constant of 1.9 and with the substrate thickness of 2.6 μm. This is given for comparison purpose, where one can notice that spacers significantly influence the transmission of CP light.

It is interesting to note that the proposed FSCMM not only converts linear polarized light into circularly polarized light but also filters out the LCP light due to its inherent handedness property. For instance, the LCP coefficients for x- and y-polarized incidences are corresponding to $T_{-x} \approx T_{-y} \approx -40$ dB at 2.5025 THz. Thus the optical isolation (difference between the RCP and LCP transmission) of the proposed FSCMM is around 35 dB at 2.5025 THz, which indicates that the proposed FSCMM has very high circular dichroism. Moreover, the proposed FSCMM is compact with a thickness of $\lambda/9$ and transverse dimension of $\lambda/4 \times \lambda/4$ at the operating wavelength of $\lambda = 119.88$ μm. Since many biological samples such as proteins, DNA and chemical species are showing differential transmission for LCP and RCP light, the filtering aspect of the proposed FSCMM is highly useful in far-infrared spectroscopy and imaging devices.

3. Mechanism of Circular Polarization Conversion and Filtering

To probe the CP conversion mechanism of the proposed FSCMM, surface current analysis is performed. For explanation purpose, the surface current distribution of mirror symmetric structure (front and back layers of FS patterns are superimposed themselves) is given at 2.5025 THz for y-polarized incident wave [see Fig. 3(a)]. It is observed that the entire mirror symmetric structure acts as an electric dipole, where the surface currents in the front (solid arrows) and back layers (dashed arrows) are oscillating symmetrically. This symmetric current distribution will only results in co-polarization transmission as the cross coupling of electromagnetic fields is absent due to mirror symmetry. This is evident from Fig. 3(b) that the co- (T_{yy}) and cross-polarization (T_{xy}) transmissions of mirror symmetric structure are -5.2 dB and -60 dB at 2.5025 THz, respectively. On the other hand, for CP conversion in CMM, it must have both T_{xy} and T_{yy} transmissions. This is possible, when CMM possesses both electric and magnetic dipole coupling interactions for linear polarization excitations.

In chiral geometries, the front and back metal layers could separately act as an electric dipole so that the entire structure resonates as a magnetic dipole due to the anti-symmetric current distribution [see the inset of Fig. 3(b)]. If the induced magnetic dipole moment is along the direction of applied electric field of the incident wave, the structure will witness the cross-polarization due to strong electromagnetic coupling. Hence, if the structure has both symmetric and anti-symmetric current contributions, it will have both co- and cross-polarization transmissions. This is evident from the surface current distribution of the FSCMM structure given in Fig. 3(c) at 2.5025 THz for y-polarized normal incident wave. The solid and dashed arrows are corresponding to the surface currents at front and back layers of FS patterns, respectively. It is noticed that different parts of the spiral rings witness both anti-symmetric and symmetric current interactions so that the cross- and co-polarized fields are induced due to electromagnetic coupling. While Fig. 3(c) explains the mechanism of cross- and co-polarized transmission, the spinning

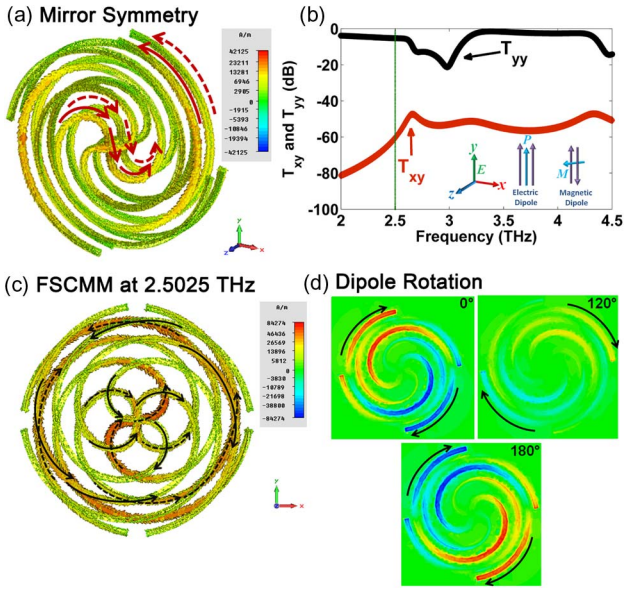

Fig. 3. (a) Surface current distribution of mirror symmetry structure at 2.5025 THz. (b) Co- (T_{yy}) and cross-polarized (T_{xy}) transmission spectra of mirror symmetry structure. The inset in (b) shows the schematic coupling scheme. (c) Surface current distribution of FSCMM structure at 2.5025 THz. The solid and dashed arrows represent the currents in front and backside of the FS layers, respectively. (d) E_z component recorded at three different phases (0°, 120°, and 180°) at 2.5025 THz. In all cases, *y*-polarized incident wave is taken for excitation.

nature of the electric dipole given in Fig. 3(d) gives the mechanism of circular dichroism in the proposed FSCMM.

Fig. 3(d) shows the E_z component along the substrate at three different phases. It is noticed that the electric dipoles are rotating clockwise as the phase is progressed. Due to this clockwise spinning of the electric dipole, LCP wave is strongly coupled to FS metal layers and it will completely dissipate inside the structure. On the other hand, RCP wave is allowed to transmit through the structure. Similarly, when a linearly polarized (LP) light is excited to FSCMM, rotated dipoles will couple to electric field of the incident light. At any point in time, the rotated dipole will trace out circular polarized light because of the spinning behavior. Thus for the given FSCMM structure, it performs three functions, namely 1) linear to circular polarization conversion (RCP), 2) transmission of RCP light under RCP excitation, and 3) complete dissipation of LCP light under LCP excitation due to handedness of FSCMM. Because of this handedness property, the structure exhibits strong circular dichroism and act as a circular polarizer.

One may also notice that in CMM based CP converters, the reverse functionality, i.e., converting circular polarization to linear polarization is not possible because of the same handedness property. For instance, as per (3), to produce linear polarized light, the structure must show equal magnitudes of RCP and LCP light so that the ellipticity is zero. However, it is noticed that the structure prohibits LCP light because of the handedness. This is a unique difference between the chiral metamaterial and conventional-material based CP converters.

By exploiting the spinning behavior of dipoles, it is also straight forward to design LCP polarizers similar to this RCP polarizer by inverting the FSCMM handedness. Thus with the proposed FSCMM structure, one can derive both LCP and RCP polarizers and selective filters for integrated THz photonic devices.

4. CP Conversion and Filtering Functionalities at Oblique Incidences

It is interesting to note from Fig. 3(c) and 3(d) that adjacent spiral rings are coupled strongly via capacitive coupling. It is visible from Fig. 3(d) that the spinning of dipoles is mediated through

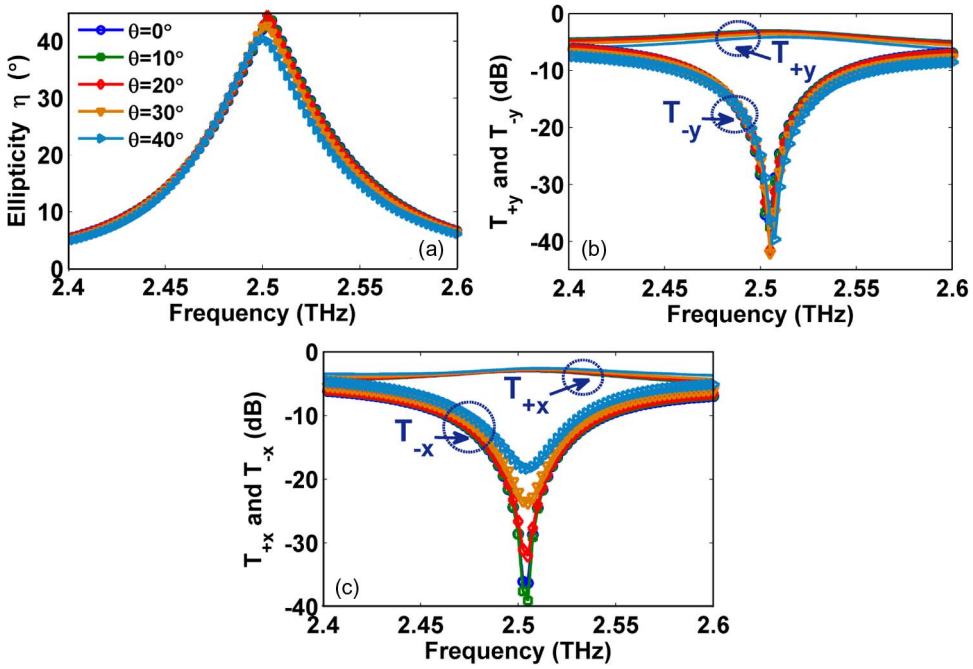

Fig. 4. CP conversion and filtering under off-normal incidences. (a) Ellipticity, (b) T_{+y} and T_{-y}, and (c) T_{+x} and T_{-x} responses with respect to incident angle variation in the range of 0° to 40°.

adjacent ring couplings. Because of this adjacent ring coupling, light with off-normal incidence can easily couple with FSCMM layers, and one can anticipate the CP conversion and filtering functionalities for oblique incidences. To verify this notion, ellipticity and CP transmission coefficients of the proposed FSCMM are computed as a function of incident angle, and their results are shown in Fig. 4. It is observed that up to 20°, ellipticity (η) response of the FSCMM indicates almost a pure circularly polarized light as their values are at the level of 44° at resonance (2.5025 THz). Beyond 20°, ellipticity is decreasing at CP resonance (At $\theta = 40°$, $\eta = 40.42°$). Although this ellipticity value is higher, it indicates a reduced optical isolation. For instance, in Fig. 4(b) under *y*-polarized excitation, it is inferred that the CP conversion results in RCP transmission of -3 dB to -3.65 dB in the incident angle range of 0° to 30°. However, higher optical isolation of 30 dB is found in the entire angular spectrum for *y*-polarized excitation.

On the other hand, for *x*-polarized excitation [see Fig. 4(c)], the RCP transmission loss is decreasing from 3 dB to 2.8 dB in the angular range of 0° to 30°. Moreover, the optical isolation and LCP loss decrease as the incident angle increases. For example, the optical isolation is reduced to the level of 20 dB at 30° for *x*-polarized excitation. This indicates that the structure is more transparent for *x*-polarized excitation and co-polarization transmission increases faster than the cross-polarization transmission under off-normal incidence of *x*-polarized light.

In the literature, the angle-invariance is possible with specific structures such as U-SRR [25] and cut wire pairs [39], [40] as they have common electric and magnetic responses under TE and TM mode excitations, respectively. However, cut wire pairs do not show higher circular dichroism and it is mostly employed as an additional structure in polarization rotator designs [39], [40] rather than CP converters for wide-angle functionality. U-SRR shows angle invariance due to the symmetry of the structure. However, to increase the optical isolation, asymmetric U-SRR [26] is preferred than symmetric U-SRR [25]. For instance, asymmetric U-SRR [26] shows optical isolation of more than 30 dB at microwave frequencies. Nevertheless, asymmetric U-SRR lacks angle invariance functionality and it will work only under *x*-polarized excitation. In line with these structures, the proposed FSCMM show wide operating angle of up to 20° with good

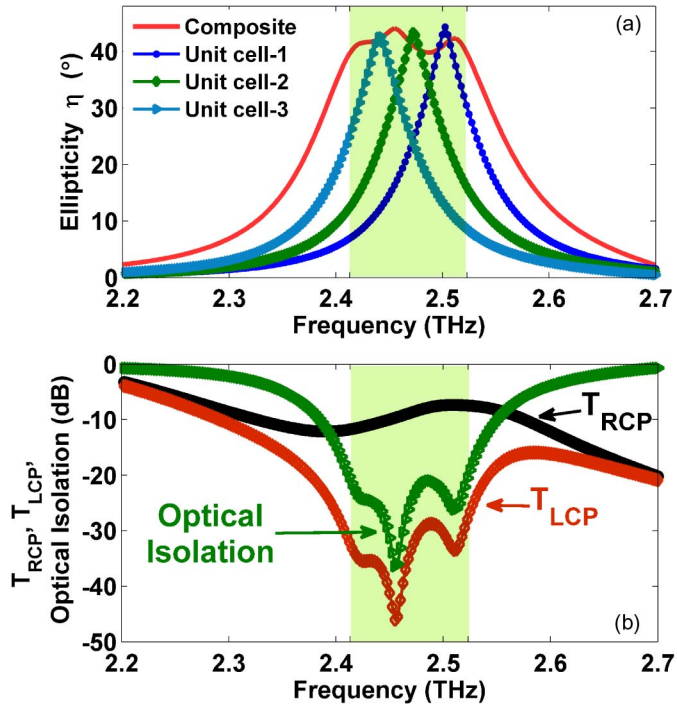

Fig. 5. Bandwidth enhancement in the composite system using three unit cells. (a) Ellipticity response of the three-unit-cell composite system and individual three unit cells. The parameters of the individual unit cells are the same as that of Fig. 1, but the spiral constants (A) of the three unit cells are varied as 4.8 μm/$\sqrt{\text{rad}}$ (unit cell-1), 4.85 μm/$\sqrt{\text{rad}}$ (unit cell-2), and 4.90 μm/$\sqrt{\text{rad}}$ (unit cell-3). (b) CP transmissions and optical isolation of the three unit-cell composite system.

optical isolation characteristics for both *x*- and *y*-polarized excitations at far-infrared frequencies. This is the desired aspect for practical implementation of CP converters in THz integrated devices.

5. Bandwidth Enhancement

The CP conversion and filtering of the proposed FSCMM follow ultra narrow band resonance, which may delimit certain practical applications. It is known that the planar structures with disconnected lattices are not suitable for wideband operation. However, one can increase the bandwidth by stacking multiple unit cells with different parameters along the direction of propagation. For example, in [27], composite system was constructed with four unit cells of CMMs by modifying the split gap parameters discretely. Nevertheless, it exhibited only a small bandwidth of 0.022 GHz for a composite thickness of $\lambda/2$, where λ is the operating wavelength. In case of the proposed FSCMM, we can increase the bandwidth up to 0.11 THz using the three unit cells with a total thickness of $\lambda/2.49$. These results are demonstrated in Fig. 5.

Since the spiraling constant of FSCMM represents the degree of wounding, it can be used to tune the resonant frequencies. In Fig. 5(a), ellipticity response of the composite system and three unit cells are shown. It is identified that the three unit cells with the spiraling constants $A = (4.8, 4.85, 4.9)$ μm/$\sqrt{\text{rad}}$ result in individual resonances at $f_{\text{resonant}} = (2.5025, 2.473, 2.442)$ THz, respectively. The composite system is a stack of these three unit cells with the polyimide spacer thickness of 17 μm. This thickness is so chosen by observing that the increase in unit cell's separation would result in enhanced bandwidth and at the same time, larger separation would decrease the magnitude of CP transmission coefficients. In addition to this, the input/output supporting spacer thicknesses are taken as 2.5 μm instead of 5 μm in the single-unit-cell system. Hence the total thickness of the composite system with three unit cells is 48.75 μm. Optical isolation and

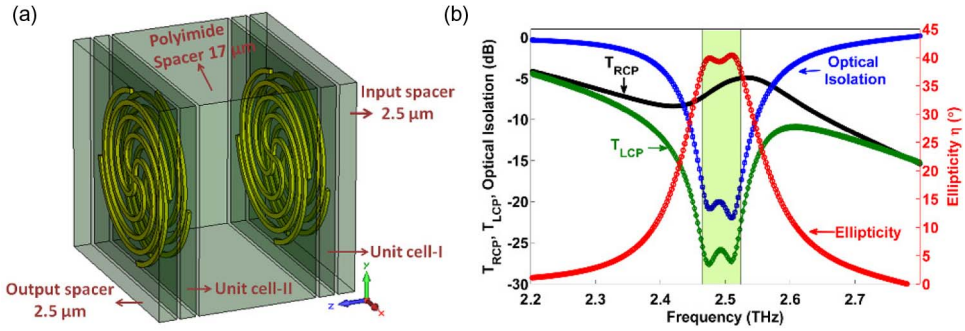

Fig. 6. (a) Composite system formed by two unit cells. Spiraling constants of the unit cells I and II are taken as $A = 4.8\ \mu\text{m}/\sqrt{\text{rad}}$ and $A = 4.85\ \mu\text{m}/\sqrt{\text{rad}}$, respectively. Total thickness of the composite system is 27.5 μm. The corresponding CP transmission and optical isolation parameters are given in (b). The shaded regime corresponds to the bandwidth of 0.058 THz.

circular polarization transmission coefficients for this composite structure are given in Fig. 5(b). The filtering functionality with 20 dB optical isolation shaded in Fig. 5(b) has a bandwidth of 0.11 THz (2.413 THz to 2.523 THz). The corresponding ellipticity bandwidth shaded in Fig. 5(a) affirms the CP conversion with the value of more than 40°, and the RCP transmission is found in the range of −7.4 dB to −11.75 dB in this shaded regime. It is clear that the transmission attenuation is the compromising factor upon bandwidth enhancement.

Suppose the composite system is made of two unit cells with the spiraling constants of $A = (4.8, 4.85)\ \mu\text{m}/\sqrt{\text{rad}}$ and the cells are separated by a polyimide spacer of 17 μm, a bandwidth of 0.058 THz (2.465 THz to 2.523 THz) is witnessed [see Fig. 6(a) and (b)]. The corresponding RCP transmission is found in the range of −7.3 dB to −4.98 dB in this specified bandwidth and the total thickness of the two-unit-cells composite is 27.5 μm at the center frequency (2.494 THz). The investigated bandwidth enhancement for the two- and three-unit-cell composite system may fulfill most of the integrated THz photonic solutions. At the same time, one may be aware that three-dimensional geometries such as helices [17]–[19] and metafoils [35] are specially intended for wideband operation due to their 3-D chirality. However, planar structures are required for the development of compact integrated components, e.g., that for THz communication and imaging.

6. Conclusion

A bilayered-twisted Fermat's spiral chiral metamaterial is proposed for the realization of far-infrared circular polarizers and handedness polarization filters. It has been demonstrated that the proposed FSCMM can convert light from linear polarization to circular polarization around 2.5 THz with a transmission loss of around 3 dB for a single-unit-cell system with polyimide spacers. The proposed single-unit-cell FSCMM can also act as an integrated handedness polarization filter with an optical isolation of 35 dB around 2.5 THz. In addition, the CP conversion and filtering functionalities of the proposed FSCMM shows a wide angle functionality up to 20° with an optical isolation of more than 25 dB for both *x*- and *y*-polarized excitations. It is further demonstrated that the three-unit-cell system shows a wide operating bandwidth of 0.11 THz with an acceptable transmission loss of CP light in the range of 7 dB to 11 dB. The transmission loss can be reduced by using low dielectric constant substrates. Moreover the clockwise and anti-clockwise FS patterns can be used to design LCP and RCP filters, respectively. In addition, the mechanism of CP conversion and filtering functionalities is explained based on surface current analysis. Finally, from the aspects of strong circular dichroism, larger optical isolation, compactness, wide-angle functionalities and bandwidth requirement, it is anticipated that the reported far-infrared circular polarization and handedness filtering based on the proposed FSCMM are useful in the domains of integrated spectroscopic devices, imaging components, and communication utilities.

References

[1] M. Tonouchi, "Cutting-edge terahertz technology," *Nat. Photon.*, vol. 1, no. 2, pp. 97–105, 2007.
[2] D. Mittleman, "Breakthroughs in terahertz science and technology in 2009," *IEEE Photon.*, vol. 2, no. 2, pp. 232–234, Apr. 2010.
[3] F. Yan, C. Yu, H. Park, E. P. J. Parrott, and E. P. MacPherson, "Advances in polarizer technology for terahertz frequency applications," *J. Infrared Millim. THz. Waves*, vol. 34, no. 9, pp. 489–499, Sep. 2013.
[4] G. Chen *et al.*, "Terahertz-wave imaging system based on backward wave oscillator," *IEEE Trans. THz Sci. Tech.*, vol. 2, no. 5, pp. 504–512, Sep. 2012.
[5] J. Shan, J. I. Dadap, and T. F. Heinz, "Circularly polarized light in the single-cycle limit: The nature of highly polychromatic radiation of defined polarization," *Opt. Exp.*, vol. 17, no. 9, pp. 7431–7439, Apr. 2009.
[6] R. M. A. Azzam and C. L. Spinu, "Achromatic angle-insensitive infrared quarter-wave retarder based on total internal reflection at the Si-SiO2 interface," *J. Opt. Soc. Amer. A, Opt. Image Sci.*, vol. 21, no. 10, pp. 2019–2022, Oct. 2004.
[7] G. P. Nordin and P. C. Deguzman, "Broadband form birefringent quarter-wave plate for the mid-infrared wavelength region," *Opt. Exp.*, vol. 5, no. 8, pp. 163–168, Oct. 1999.
[8] N. Amer, W. C. Hurlbut, B. J. Norton, Y.-S. Lee, and T. B. Norris, "Generation of terahertz pulses with arbitrary elliptical polarization," *Appl. Phys. Lett.*, vol. 87, no. 22, 2005, Art. ID. 221111.
[9] P. L. Richards and G. E. Smith, "Far-infrared circular polarizer," *Rev. Sci. Inst.*, vol. 35, no. 11, p. 1535, 1964.
[10] L. Young, L. A. Robinson, and C. A. Hacking, "Meander-line polarizer," *IEEE Trans. Antennas Propag.*, vol. AP-21, no. 3, pp. 376–378, May 1973.
[11] A. C. Strikwerda *et al.*, "Comparison of birefringent electric split-ring resonator and meanderline structures as quarter-wave plates at terahertz frequencies," *Opt. Exp.*, vol. 17, no. 1, pp. 136–149, Jan. 2009.
[12] T. Niemi, A. O. Karilainen, and A. Tretyakov, "Synthesis of polarization transformers," *IEEE Trans. Antennas Propag.*, vol. 61, no. 6, pp. 3102–3111, Jun. 2013.
[13] Y. Svirko, N. Zheludev, and M. Osipov, "Layered chiral metallic microstructures with inductive coupling," *Appl. Phys. Lett.*, vol. 78, no. 4, pp. 498–500, 2001.
[14] A. Papakostas, A. Potts, D. M. Bagnall, S. L. Prosvirnin, H. J. Coles, and N. I. Zheludev, "Optical manifestations of planar chirality," *Phys. Rev. Lett.*, vol. 90, no. 10, 2003, Art. ID. 107404.
[15] K. F. Lindman, "Uber eine durch ein isotropes system von spiralformigen resanotoren erzeugte rotationpolarisation der electromagnetischen wellen," *Annalen der Phys.*, vol. 63, no. 4, pp. 621–644, 1920.
[16] M. G. Silveririnha, "Design of linear-to-circular polarization transformers made of long densely packed metallic helices," *IEEE Trans. Antennas Propag.*, vol. 56, no. 2, pp. 390–401, Feb. 2008.
[17] J. K. Gansel *et al.*, "Gold helix photonic metamaterial as broadband circular polarizer," *Science*, vol. 325, no. 5947, pp. 1513–1515, Sep. 2009.
[18] S. Li, Z. Yang, J. Wang, and M. Zhao, "Broadband terahertz circular polarizers with single- and double-helical array metamaterials," *J. Opt. Soc. Amer. A, Opt. Image Sci.*, vol. 28, no. 1, pp. 19–23, Jan. 2011.
[19] Z. Zhao *et al.*, "High extinction ratio circular polarizer with conical double-helical metamaterials," *J. Light. Tech.*, vol. 30, no. 15, pp. 2442–2446, Aug. 2012.
[20] M. Saba *et al.*, "Circular dichroism in biological photonic crystals and cubic chiral nets," *Phys. Rev. Lett.*, vol. 106, no. 10, Mar. 2011, Art. ID. 103902.
[21] M. Thiel, G. V. Freymann, and M. Wegener, "Layer-by-layer three-dimensional chiral photonic crystals," *Opt. Lett.*, vol. 32, no. 17, pp. 2547–2549, Sep. 2007.
[22] S. Takahashi *et al.*, "Circular dichroism in a three-dimensional semiconductor chiral photonic crystal," *Appl. Phys. Lett.*, vol. 105, no. 5, 2014, Art. ID. 051107.
[23] M. Theil, M. S. Rill, G. V. Freymann, and M. Wegener, "Three-dimensional bi-chiral photonic crystals," *Adv. Mat.*, vol. 21, no. 46, pp. 4680–4682, Jul. 2009.
[24] M. Nagai *et al.*, "Achromatic THz wave plate composed of stacked parallel metal plates," *Opt. Lett.*, vol. 39, no. 1, pp. 146–149, Jan. 2014.
[25] Z. Li *et al.*, "Chiral metamaterials with negative refractive index based on four U split ring resonators," *Appl. Phys. Lett.*, vol. 97, no. 8, 2010, Art. ID. 081901.
[26] M. Mutlu, A. E. Akosman, A. E. Serebryannikov, and E. Ozbay, "Asymmetric chiral metamaterial circular polarizer based on four U-shaped split ring resonators," *Opt. Lett.*, vol. 36, no. 9, pp. 1653–1655, May 2011.
[27] Y. Ye, X. Li, F. Zhuang, and S.-W. Chang, "Homogeneous circular polarizers using a bilayered chiral metamaterial," *Appl. Phys. Lett.*, vol. 99, no. 3, 2011, Art. ID. 031111.
[28] S. Yan and G. A. E. Vandenbosch, "Compact circular polarizer based on chiral twisted double split-ring resonator," *Appl. Phys. Lett.*, vol. 102, no. 10, 2013, Art. ID. 103503.
[29] H. L. Zhu, S. W. Cheung, K. L. Chung, and T. I. Yuk, "Linear-to-circular polarization conversion using metasurface," *IEEE Trans. Antennas Propag.*, vol. 61, no. 9, pp. 4615–4623, Sep. 2013.
[30] H.-X. Xu, G.-M. Wang, M. Q. Qi, T. Cai, and T. J. Cui, "Compact dual-band circular polarizer using twisted Hilbert-shaped chiral metamaterial," *Opt. Exp.*, vol. 21, no. 21, pp. 24 912–24 921, Oct. 2013.
[31] L. M. Lopez, J. R. Cuevas, J. I. M. Lopez, and A. E. Martynyuk, "A multilayer circular polarizer based on bisected split-ring frequency selective surfaces," *IEEE Antenna Wire. Propag. Lett.*, vol. 13, pp. 153–156, Jan. 2014.
[32] H.-X. Xu, G.-M. Wang, M. Q. Qi, and T. Cai, "Dual-band circular polarizer and symmetric spectrum filter using ultra-thin compact chiral metamaterial," *Prog. Electromagn. Res.*, vol. 143, pp. 243–261, 2013.
[33] G. Kenanakis *et al.*, "Flexible chiral metamaterials in the terahertz regime: A comparative study of various designs," *Opt. Mater. Exp.*, vol. 2, no. 12, pp. 1702–1712, Dec. 2012.
[34] P. Zhang *et al.*, "Giant circular polarization conversion in layer-by-layer nonchiral metamaterial," *J. Opt. Soc. Amer. A, Opt. Image Sci.*, vol. 30, no. 9, pp. 1714–1718, Sep. 2013.

[35] J. Wu *et al.*, "Chiral metafoils for terahertz broadband high-contrast flexible circular polarizers," *Phys. Rev. App.*, vol. 2, no. 1, 2014, Art. ID. 014005.
[36] Y. Zhao, M. A. Belkin, and A. Alu, "Twisted optical metamaterials for planarized ultrathin broadband circular polarizers," *Nat. Commun.*, vol. 3, p. 870, 2012.
[37] H. Tao *et al.*, "Terahertz metamaterials on free-standing highly-flexible polyimide substrates," *J. Phys. D: Appl. Phys.*, vol. 41, no. 23, 2008, Art. ID. 232004.
[38] D. A. Doane and P. D. Franzon, *Multichip Module Technologies and Alternatives: The Basics*. New York, NY, USA: Springer, 1993, Ch-8. 311–347.
[39] C. Xi, "Terahertz angle-insensitive 90 polarization rotator using chiral metamaterial," *Phys. B*, vol. 442, pp. 83–86, Aug. 2013.
[40] K. Song *et al.*, "90 polarization rotator with rotation angle independent of substrate permittivity and incident angle using a composite chiral metamaterial," *Opt. Exp.*, vol. 21, no. 6, pp. 7439–7446, Mar. 2013.